Surface Science 248 (1991) 45–56
North-Holland

A vibrational spectroscopy study of CH_3COOH, CH_3COOD and $^{13}CD_3COOH(D)$ adsorption on Pt(111)

I. Surface dimer formation and hydrogen bonding

Quanyin Gao and John C. Hemminger

Institute for Surface and Interface Science and Department of Chemistry, University of California, Irvine, CA 92717, USA

Received 8 August 1990; accepted for publication 20 November 1990

Acetic acid (CH_3COOH, CH_3COOD and $^{13}CD_3COOH(D)$) adsorption on Pt(111) at 168 K has been studied as a function of surface coverage with HREELS. At low acetic acid dosages ($\theta < 0.3$), dissociative adsorption occurs forming a surface acetate species with an η^2(O, O)-CH_3COO configuration in a C_s symmetry. Further dissociative adsorption as $CO_{(a)}$, $O_{(a)}$ and $CH_{x(a)}$ with $x = 1$–2 is observed for very low acetic acid dosages ($\theta \sim 0.2$ or less). The formation of $HCOO_{(a)}$ or $CH_{3(a)}$ from acetic acid adsorption is ruled out based on the absence of their characteristic vibrational modes. Molecular adsorption occurs at moderate acetic acid dosages ($\theta \sim 0.5$ or above) with a finger print peak at ~ 932 cm^{-1} for CH_3COOH and $^{13}CD_3COOH$ adsorbates. This mode corresponds to a well documented γ_{OH} mode of the acetic acid dimer. Hydrogen bonding between neighboring acetic acid molecules is responsible for the stabilization of the acetic acid hydroxyl group. The adsorbed acetic acid configuration is proposed to be a cyclic dimer with the dimer ring nearly parallel to the plane of metal surface. Quantitative correlations have been developed between the frequency of the γ_{OH} mode and the strength (ΔH) and bond length ($R_{O\ldots O}$) of the hydrogen bond for a number of carboxylic acid dimers. Using these correlations from the literature our data can be used to estimate the hydrogen bond energy for acetic acid dimer on Pt(111) to be ~ 7.3 kcal/mol with a corresponding estimate of the $R_{O\ldots O}$ distance of ~ 2.68 Å.

1. Introduction

Acetic acid has been known to form hydrogen-bonded cyclic dimers in the gas phase [1]. In the liquid phase, both cyclic and chain types of dimers are considered possible while in the solid crystal, infinite chains of hydrogen bonded structure of acetic acid have been reported [2,3]. As a continued effort to study the hydrogen bonding effects on surface chemistry, acetic acid has been chosen here following our studies of formamide surface chemistry. For the latter, hydrogen bonding and its influence on surface chemistry has been investigated on both Ni(111) [4] and Pt(111) [5].

The adsorption of acetic acid on transition metal surfaces has been the subject of several previous experimental investigations [6–11]. On Pt(111), a previous study has shown acetate species formation by oxygen pre-adsorption on the surface at low temperature [6]. The acetate species has also been reported on Cu(100) [7,8] and Al(111) [11] at low acetic acid exposures. A hydrogen-bonded dimer form of acetic acid has been observed on Al(111) at high exposure (1.5×10^{17} molecules/cm^2), which is attributed to the physisorbed acetic acid molecules, from which we deduced that the adsorption is multilayer.

In our study, a systematic investigation is conducted to find the coverage dependence of hydrogen bonded species and the role it plays in surface chemistry. In order to have a clear vibrational mode assignment, isotopically labeled molecules of CH_3COOD and $^{13}CD_3COOH(D)$ are used in addition to CH_3COOH for the HREELS and TDS experiments.

2. Experimental section

The experiments were performed in a two-level UHV chamber with a base pressure of 1×10^{-10}

Torr. The upper level is equipped with low-energy electron diffraction (LEED) optics, Auger electron spectrometer with cylindrical mirror analyzer, quadrupole mass spectrometer, ion sputtering gun and sample doser. The lower level houses the high-resolution electron energy loss spectrometer (HREELS).

An LK2000-14-R HREEL spectrometer was used for the vibrational analysis with a routine resolution of about 30 cm^{-1} (FWHM of the elastic peak) for the clean Pt(111) surface. The spectral resolution did not degrade with acetic acid dosages within a monolayer coverage. A typical elastic beam counting rate at this resolution is about 10^5–10^6 counts/s. From LEED measurements, no surface ordering was found for acetic acid adsorption on Pt(111) which indicates, given the high performance quality of the HREEL spectrometer, that the system studied is a *disordered overlayer*. The incident electron beam energy used is about 7 V and the incident angle is 60° from the surface normal of the Pt(111) sample. Unless mentioned otherwise in the figure, the spectra were recorded in the specular direction.

The Pt(111) surface was oriented to within ±0.5° of the desired (111) plane confirmed by both Laue X-ray diffraction and LEED. The surface cleanliness, following argon ion bombardments and oxygen treatments, was checked by both Auger electron spectroscopy (AES) and HREELS.

CH_3COOH, CH_3COOD and $^{13}CD_3COOH(D)$ were obtained from Aldrich. The purity of CH_3COOH is 99.7%. CH_3COOD has 98 at% D isotope purity and $^{13}CH_3COOH(D)$ has 97.2 at% ^{13}C, 97.27 at% D for the methyl group and 43 at% D for the hydroxyl group. They are further purified in the gas dosing line by several freeze–pump–thaw cycles. A doser was used for acetic acid adsorption onto the front face of the cooled Pt(111) crystal. The doser consists of a 1/4 inch o.d. stainless steel tube whose orifice was located approximately 1 cm from the crystal surface. Reproducing the acetic acid coverages was accomplished by immediately rotating the crystal out of the acetic acid dosing beam after the preset dosing time. The effectiveness of dosing in this manner was confirmed by monitoring the reproducibility of the HREELS and the thermal desorption spectroscopy (TDS).

3. Results

3.1. Adsorption of CH_3COOH on Pt(111) at 168 K

A set of Auger peak-to-peak ratios of C_{273}/Pt_{237} were measured as a function of CH_3COOH dosage and the plot is shown in fig. 1. This plot shows an abrupt change in slope at ~ 20 s exposure time. The turning point for the slope change is assigned to monolayer exposure ($\theta = 1$) to establish a relative exposure scale. Our TDS results are consistent with this assignment which showed saturation exposure at this acetic acid dosage before the multilayer desorption peaks appear [12].

For the different CH_3COOH dosages shown in fig. 1, corresponding HREEL spectra have been taken. Fig. 2 is a plot of some of these HREEL spectra measured at 168 K as a function of increasing CH_3COOH exposure. At an initial small CH_3COOH dosage ($\theta \sim 0.03$) five vibrational modes are observed at 467, 661, 768, 1398 and 2057 cm^{-1}, as shown in fig. 2a. After increasing the CH_3COOH dosage to $\theta \sim 0.19$, five more peaks occur at 302, 913, 1000, 2930 and 2988 cm^{-1} (fig. 2b). Substantial peak broadening as a function of increasing dosage is observed for the band at

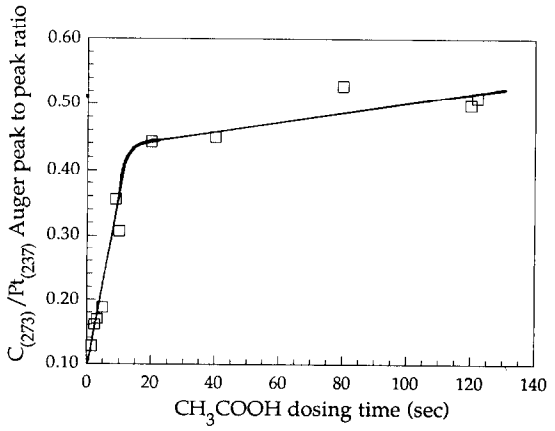

Fig. 1. Acetic acid Auger uptake curve, the acetic acid adsorption temperature is 168 K, the chamber background pressure is 5×10^{-10} Torr when the dosing beam in on.

about 2940 cm^{-1} (figs. 2d–2h). At $\theta \sim 0.30$ dosage (fig. 2c), the previous peak at 2048 cm^{-1} has disappeared accompanied by a drop of intensity of the 467 cm^{-1} peak, and a new peak is observed at 874 cm^{-1} (fig. 2c) which later shifts to about 932 cm^{-1} with increasing coverage. A weak peak at 1660 cm^{-1} appears when CH_3COOH dosage is above $\theta \sim 0.5$ (figs. 2d–2h). In fig. 2f, a peak at 219 cm^{-1} is observed. With larger exposure, this peak is not detected which could be caused by the loss of resolution of this band with the tail of the elastic peak since the instrumental resolution decreases when large exposures are used (before fig. 2f, FWHM is about 30 cm^{-1} for the elastic peak, after fig. 2f, FWHM increases to ~ 40 cm^{-1}). In all spectra shown in fig. 2, the dominant peak is at ~ 1400 cm^{-1}. The second dominant peak is at ~ 671 cm^{-1} for CH_3COOH dosages below $\theta \sim 0.5$. When the acetic acid dosage exceeds $\theta \sim 0.5$ the peak at 932 cm^{-1} becomes the second dominant peak.

A series of CH_3COOH spectra with relative exposure of 7.5 measured at 168 K are plotted out as a function of off-specular scattering angle (fig. 3). At 10° off-specular (fig. 3d), a peak splitting is observed clearly at 605 and 698, 910 and 1003, 1318 and 1400 cm^{-1} as well as a peak intensity enhancement for the 2927 cm^{-1} band. With small initial exposure of $\theta \sim 0.19$, the off-specular spectrum is shown in fig. 4, in which only one peak splitting is observed at 1340 and 1400 cm^{-1} (fig. 4b).

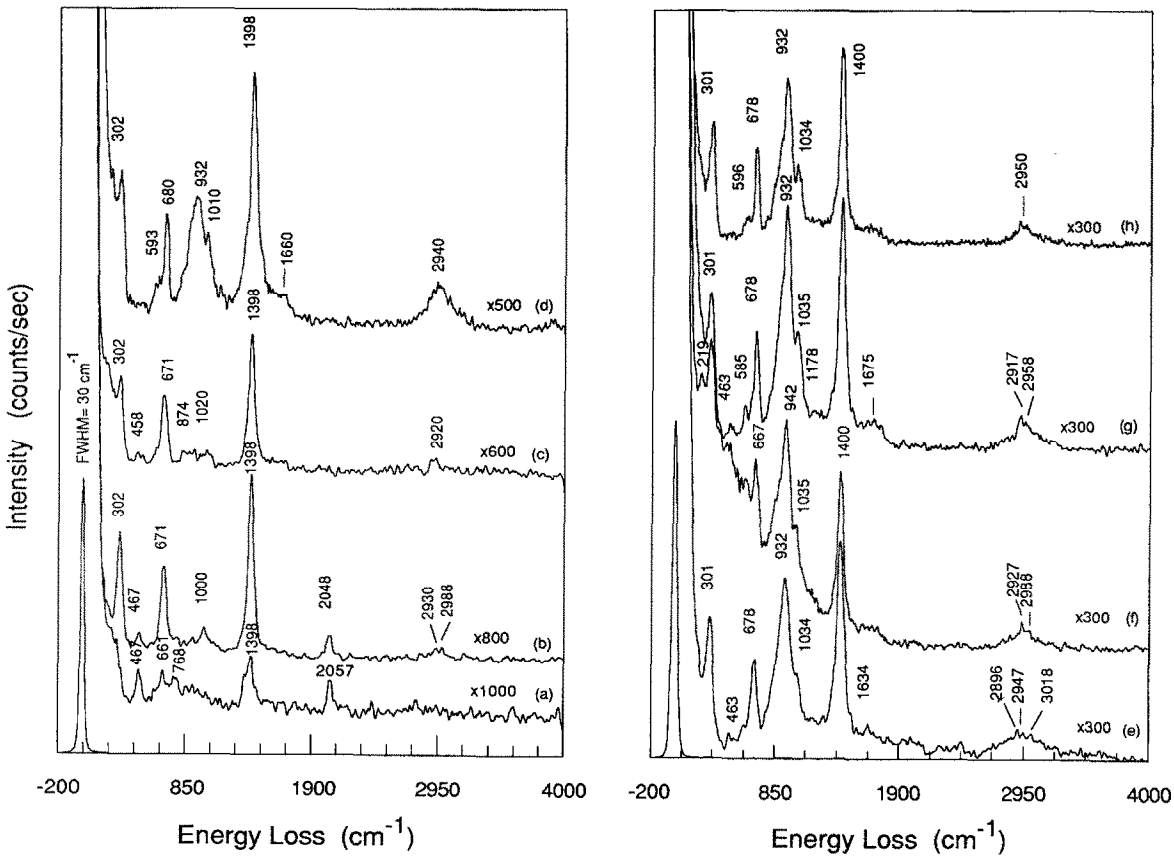

Fig. 2. Coverage dependent HREEL spectra of CH_3COOH on Pt(111) with acetic acid adsorption at 168 K and dosages of (a) $\theta \sim 0.03$, (b) $\theta \sim 0.19$, (c) $\theta \sim 0.30$, (d) $\theta \sim 0.50$, (e) $\theta \sim 0.63$, (f) $\theta \sim 1.25$, (g) $\theta \sim 2.5$, (h) $\theta \sim 7.5$.

3.2. CH_3COOD adsorption on Pt(111) at 168 K

Three exposures of CH_3COOD have been recorded and the HREEL spectra are shown in fig. 5. At low exposure ($\theta \sim 0.63$), vibrational peaks are observed at 290, 464, 565,680, 836, 942, 1029, 1156, 1388, 1660, 2038, 2910, 2979 and 3037 cm^{-1} (fig. 5a), in which the dominant peak is at 1388 cm^{-1} and the second dominant peak is at 680 cm^{-1}. These two peaks change relative intensity at larger exposures as shown in figs. 5b and 5c where the 687 cm^{-1} peak becomes the strongest peak. Three peaks at 2910, 2979 and 3037 cm^{-1} become less well resolved and the peaks at 2038 and 464 cm^{-1} disappear with larger dosages (figs. 5b and 5c).

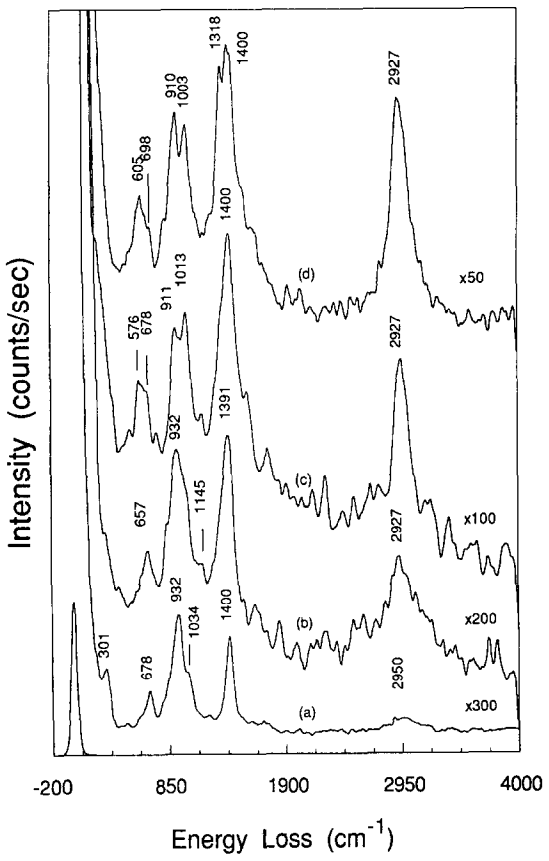

Fig. 3. Off-specular spectra of CH_3COOH adsorption on Pt(111) at 168 K with a dosage of $\theta \sim 7.5$. Off-specular angles are: (a) 0°, (b) 3°, (c) 5°, (d) 10°.

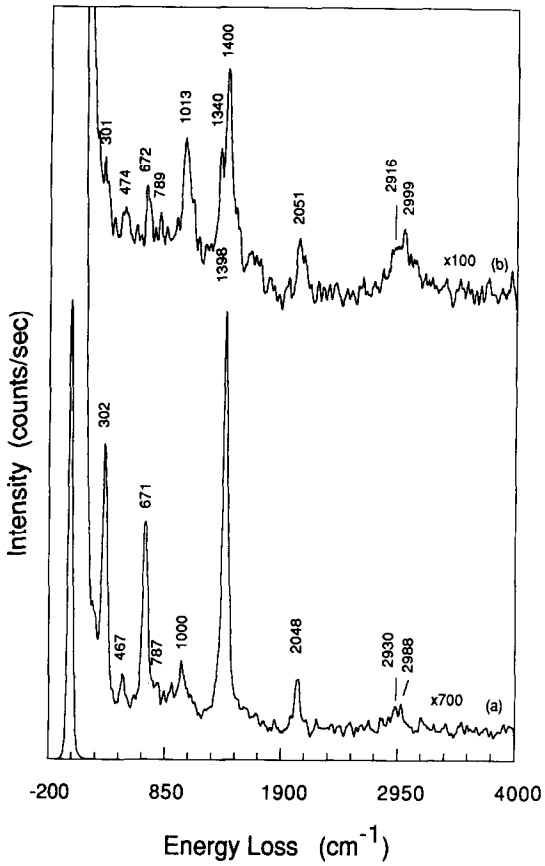

Fig. 4. Off-specular spectra of CH_3COOH adsorption on Pt(111) at 168 K with a dosage of $\theta \sim 0.19$. (a) On-specular, (b) 5° off-specular.

3.3. $^{13}CD_3COOH$ adsorption on Pt(111) at 168 K

The isotopically labeled molecule $^{13}CD_3COOH(D)$ has been studied with three relative exposures of 0.31, 1.25 and 3.75. The HREEL spectra are shown in figs. 6a–6c. At low dosages, peaks are observed at 225, 428, 661, 768, 903, 1049, 1176, 1388, 1602, 1902, 2058, 2203 and 2261 cm^{-1} (fig. 6a). With larger dosages, the peaks at 428, 1902 and 2058 cm^{-1} disappear (figs. 6b and 6c). The strongest peak is at 388 cm^{-1} with low dosage (fig. 6a) and at 661 cm^{-1} with larger dosages (figs. 6b and 6c).

4. Discussion

4.1. Acetic acid dosage versus surface coverage at 168 K

In fig. 1, the Auger peak intensity ratio for C_{273}/Pt_{273} is plotted out as a function of increasing CH_3COOH dosage. A slope change has been observed at a relative exposure of 1.0. After this point, the C_{273}/Pt_{237} ratio grows very slowly with CH_3COOH dosage. This can be understood as follows. The CH_3COOH dosage below 1.0 is in the first monolayer coverage region so that the CH_3COOH molecules have high sticking probabilities due to the chemical interaction between the acetic acid adsorbate and the Pt(111) substrate. At about an exposure of 1.0, a monolayer of

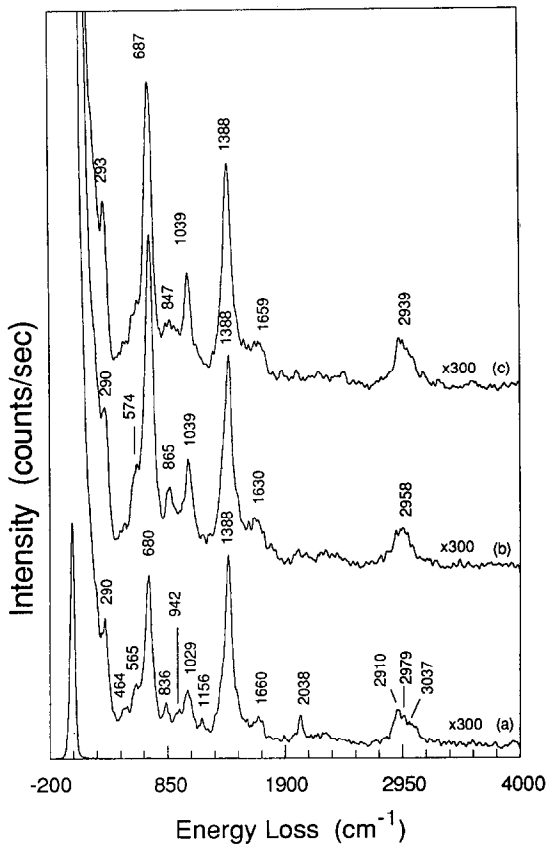

Fig. 5. Coverage dependent HREEL spectra of CH_3COOD on Pt(111) with acetic acid dosages of (a) $\theta \sim 0.63$, (b) $\theta \sim 1.25$, and (c) $\theta \sim 3.75$.

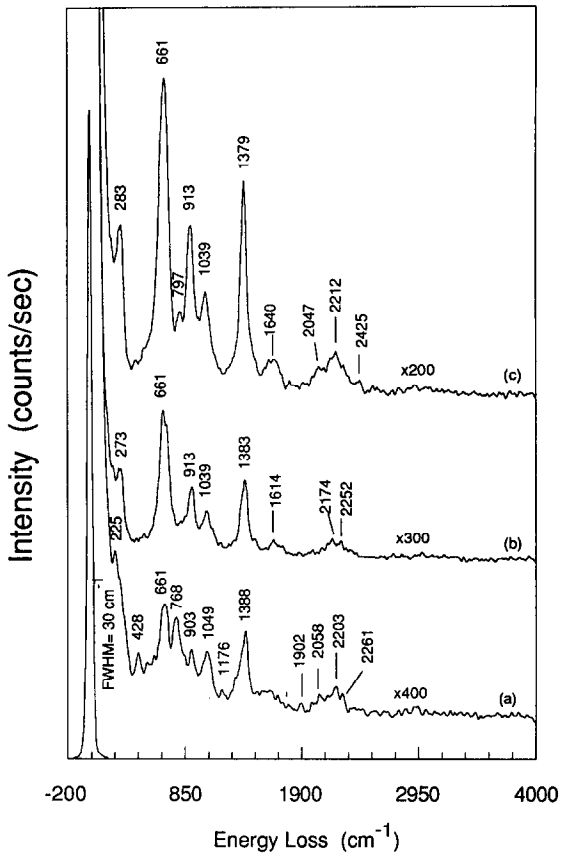

Fig. 6. Coverage dependent HREEL spectra of $^{13}CD_3COOH(D)$ adsorption on Pt(111) at 168 K with acetic acid dosages of (a) $\theta \sim 0.3$, (b) $\theta \sim 1.25$, and (c) $\theta \sim 3.75$.

CH_3COOH is formed on the surface. After this point, the CH_3COOH molecules have lower sticking probabilities due to the weak van der Waals interaction between the acetic acid and the acetic acid covered substrate. This is indicated by a very slow increase of the C_{273}/Pt_{237} peak-to-peak ratio as a function of dosage. The high slope region corresponds to a chemisorption process while the small slope region corresponds to a physisorption process. The difference in adsorption nature is the cause for the change in sticking probabilities and thus, for the change of the slope in fig. 1.

In our acetic acid adsorption experiments, the adsorption temperature of 168 K is a little high for physisorbed multilayers to be stable which is observed from our TDS experiments [12]. The possible electron beam induced desorption has

been considered during Auger data collection and efforts have been made to reduce this effect by using a relatively low beam voltage (1 kV) and a low filament emission current (0.5 mA). With these electronic parameters the current measured at the crystals is ~ 4 μA. However, the nature of the bonding that changes the acetic acid sticking probability will not be altered given the presence of the electron beam induced desorption process. In our latter discussion, a coverage of $\theta = 1.0$ will refer the point at which this dramatic change of slope in fig. 1 is obtained. If we assume a sticking probability of CH_3COOH molecules for chemisorption to be one and 1 langmuir (1×10^{-6} Torr s) as the monolayer exposure, we estimate that our doser for acetic acid adsorption has a pressure enhancement factor of about 125. This CH_3COOH dosage and the surface coverage correlation is further supported by HREELS results. In fig. 2f, the acetic acid dosage is 1.25 which is a little over monolayer exposure and the lattice mode of multilayer acetic acid at 219 cm^{-1} is observed. Below this dosage, we have not observed this mode which agrees that at 1.25 dosage multilayer starts to form. This mode for larger dosages is hard to detect due to the broadened elastic peak and its high background tail which interferes strongly with this low frequency mode at 219 cm^{-1}.

4.2. Acetate formation on Pt(111) at 168 K

As we can see from fig. 2, at low acetic acid dosage ($\theta \sim 0.2$), the adsorption of CH_3COOH is dissociative. This is characterized by the lack of O–H related modes such as the stretching vibrational mode (ν_{OH} is at 3640 cm^{-1} for CH_3COOH monomer [13]), O–H in plane bending mode (δ_{OH} is at 1176 cm^{-1} for CH_3COOH monomer [13]) as well as O–H out of plane bending mode (γ_{OH} is 650 cm^{-1} for CH_3COOH monomer [14]). The absence of these O–H bond related vibrational modes in the HREEL spectra strongly suggests that the O–H bond of the acetic acid molecule is cleaved upon adsorption on Pt(111) at 168 K, resulting in the acetate formation on Pt(111). The acetate species has also been identified for oxygen pre-exposed Pt(111) by Avery [6] in which it was intended to generate acetate species by enhancing the Bronsted basicity of the metal surface with pre-adsorption of oxygen. Our results indicate that even without oxygen pre-adsorption, the Pt surface has enough basicity to react with acetic acid forming surface acetate. The acetate species has also been reported by Chen et al. on Al(111) [11], by Bowker et al. on Cu(110) [10] and by Sexton on Cu(111) [7,8].

The comparison of the vibrational frequencies of the acetate species is given in table 1 in which our result and the results from aqueous solution, Al(111), Cu(100) and oxygen pre-adsorbed Pt(111) are listed. The assignments for surface acetate vibrational modes on Pt(111) at 168 K are as follows: C–H stretching (ν_{CH}) at 2988 ~ 2930, symmetric COO stretching (ν_{sCOO}) at 1398 cm^{-1}, CH umbrella bending mode (δ_{CH_3}) at 1340 cm^{-1} (resolved from ν_{sCOO} mode at 1398 cm^{-1} with off-specular observation fig. 4b), C–C stretching (ν_{CC}) at 1000 cm^{-1}, in plane COO bending (δ_{COO})

Table 1
Acetate vibrational mode assignments

	CH_3COO^- [32]	(CD_3COO^-)	Cu(100) [8]		Al(111) [11]		Pt(111) [6]	Pt(111) [this work]	
ν_{CH}	2935	(2111)	3000	(2218)	3025	(2260)	–	2930–2988	(2261, 2203)
ν_{aCOO}	1556	(1545)	–	–	–	–	–	–	–
ν_{sCOO}	1413	(1406)	1434	(1413)	1470	(1470)	1400	1398	(1388)
δ_{CH_3}	1344	(1085)	–	–	–	–	–	1340[os,a)]	(903)
ν_{C-C}	926	(883)	1041	(1061)	1055	(1070)	–	1000	(1049)
δ_{COO}	650	(619)	677	(648)	695	(655)	665	671	(661)
ρ_{COO}	471	(419)	–	–	–	–	–	463	(428)
ν_{M-O}	–	–	339	(308)	425	(410)	300	302	(225)

[a)] os: off-specular observation.

mode at 671 cm^{-1} and substrate platinum–oxygen of the acetate stretching vibration (ν_{Pt-O}) at 302 cm^{-1}. The strong intensity for ν_{sCOO}, δ_{COO} and ν_{Pt-O} in the specular direction indicates that these modes are dipole active. The absence of ν_{aCOO} in the specular spectra (figs. 2a–2c) indicates that this vibrational mode is dipole forbidden on the metal surface. This could be accounted for by an adsorption of a bidentate acetate $\eta^2_{(O,O)}$-CH_3COO which is in a C_s symmetry. As explained by Sexton [7–8] and Chen et al. [11], this configuration would given ν_{sCOO}, δ_{COO} and ν_{Pt-O} modes large dynamic dipole components perpendicular to the plane of the metal surface and hence strong on-specular peak intensities. The ν_{aCOO} vibrational mode, however, will be weak since its dynamic dipole has little component perpendicular to the plane of the metal surface. These are consistent with the surface dipole selection rule, i.e., only those vibrations with a nonzero dynamic dipole component perpendicular to the plane of metal surface will be observed with dipole scattering. The off-specular scattering is known to enhance the impact scattering mechanism. The ν_{CH} and δ_{CH_3} peaks are examples here. The spectra shown in fig. 4a indicates that the ν_{CH} mode at 2900–3000 cm^{-1} and the δ_{CH_3} mode at $\sim$1340 cm^{-1} are enhanced by off-specular observation. These two modes are thus considered to be impact-scattering enhanced.

Apart from the acetate formation as discussed above, further dissociation of CH_3COOH to $CO_{(a)}$ is observed as well. In figs. 2a and 2b, ν_{CO} and ν_{Pt-CO} are observed at 2057 and 467 cm^{-1}, respectively. These two peaks disappear for larger dosages (figs. 2c and 2e). The small peak at $\sim$413 cm^{-1} in figs. 2e–2g is the out-of-plane bending mode of the COO group (ρ_{COO}) in molecularly adsorbed acetic acid molecules. The formation of the adsorbed CO is clearly from the dissociation of CH_3COOH rather than from the chamber background CO adsorption since no such modes are observed prior to CH_3COOH adsorption. Our temperature dependent HREELS and thermal desorption results also indicate that CO is a direct dissociation product from CH_3COOH at elevated temperatures [12]. The presence of a $CO_{(a)}$ fragment from CH_3COOH dissociation hints that further bond scission other than the O–H bond is possible at this adsorption temperature of 168 K. Apparently, the C–C bond and C–O bond are broken to form $CO_{(a)}$. We have ruled out the presence of $HCOO_{(a)}$ and $CH_{3(a)}$ species. For the $HCOO_{(a)}$ species, the literature indicates that the ν_{sCOO} mode is in the range of 1300–1350 cm^{-1} [15–22] while the $CH_3COO_{(a)}$ species has ν_{sCOO} at 1398–1470 cm^{-1} [6–8,11]. This is about 100 cm^{-1} higher than the corresponding mode in $HCOO_{(a)}$. The δ_{COO} mode is at 760–785 cm^{-1} for the $HCOO_{(a)}$ species while the $CH_3COO_{(a)}$ species have δ_{COO} at 650–675 cm^{-1} which about 100 cm^{-1} lower than the corresponding mode in $HCOO_{(a)}$. The lack of a δ_{sCH_3} vibration, which has been reported to be a strong mode at $\sim$1200 cm^{-1} for $CH_{3(a)}$ [23,24], indicates that the surface $CH_{3(a)}$ species is possibly not stable in our experimental conditions. The surface $CH_{2(a)}$ group has been reported on Ru(001) [25] with strong peaks at 2940 (ν_{sCH_2}) and 1450 cm^{-1} (δ_{sCH_2}). In fig. 2b, modes at 2930, 2988 and 1398 cm^{-1} may have contributions from surface $CH_{2(a)}$ species. $CH_{(a)}$ species may also be present since this species gives ν_{CH} modes at 3050 cm^{-1} and δ_{CH} mode at 770 cm^{-1} [26,27]. We have observed weak peaks at 2988 and 768 cm^{-1} (figs. 2a and 2b) which could be from $CH_{(a)}$. The peak at 768 cm^{-1} in fig. 2a is also present with $^{13}CD_3COOH(D)$ adsorption at low dosage (fig. 6a), which indicates that apart from the possible $CH_{(a)}$ other species may have contributions to this peak. The most probable one is $O_{(a)}$ since this species is also a counter part of $CO_{(a)}$ from CH_3COOH dissociative adsorption, and on Pt(111) this mode has been observed at 750–800 cm^{-1} with Ca impurities [28]. Thus, we observe CH_3COOH dissociatively adsorbed on Pt(111) at low dosages forming surface acetate ($CH_3COO_{(a)}$) and surface $H_{(a)}$. Acetate species could further decompose to $CO_{(a)}$, $O_{(a)}$ and CH_x species with $x = 1$–2 at very low acetic acid dosage.

4.3. Molecular adsorption of acetic acid on Pt(111) at 168 K

Nondissociative molecular adsorption of acetic acid occurs after the Pt(111) surface is passivated by the species from acetic acid dissociation. When

the acetic acid dosages exceed $\theta \sim 0.5$ new features of the vibrational spectra grow in at 932 cm^{-1} for $CH_3COOH/Pt(111)$ (figs. 2d and 2d–2h) and at 913 cm^{-1} for $^{13}CD_3COOH(D)/Pt(111)$ (figs. 6b and 6c). With more exposure, the peak intensity increases and exceeds the δ_{COO} mode (~ 678 cm^{-1}) as the second dominant peak (figs. 2d–2h). The width of this peak also increases as a function of increasing dosage. All these phenomena are not observed for the deuterium-substituted OH group molecule CH_3COOD in figs. 5a–5c. Thus, we conclude that peaks at 932 cm^{-1} for CH_3COOH adsorbate and 913 cm^{-1} for $^{13}CD_3COOH(D)$ adsorbates are related to the hydroxyl group (OH). After literature studies it turns out that this peak originates from the out of plane bending mode for the OH group (γ_{OH}) from acetic acid cyclic dimers which we will discuss in detail later. We would like to point out here that due to the strong hydrogen bonding between neighboring acetic acid molecules and possible between acetic acid and acetate species, the ν_{OH} mode is no longer characteristic for molecular adsorption identification. The "free" OH stretching frequency (ν_{OH}) for the acetic acid molecule in the gaseous state at 430 K is observed at 3583 cm^{-1} [29]. It decreases to a broad peak near 2900 cm^{-1} in the acetic acid crystal near 90 K [29] and is hard to differentiate from the C–H stretching peak which also falls in this region. The ν_{OH} can vary from 2900 to 3100 cm^{-1} for liquid CH_3COOH with temperature and solvents due to their influence on the strength of hydrogen bonding [30]. It is thus not surprising that different ν_{OH} frequencies have been reported in the literature. However, the γ_{OH} mode is found to be characteristic [31] and thus is used here as an indicator of the presence of molecular adsorption. The γ_{OH} mode is observed with a dosage of $\theta \sim 0.5$ (fig. 2d). With the presence of the γ_{OH} mode at ~ 932 cm^{-1}, the peak in the 2900–3020 cm^{-1} region becomes broadened (figs. 2d–2g) which we assume is due to contributions from ν_{H-O-H} in this region. On the Al(111) surface ν_{H-O-H} has been observed at 2740 cm^{-1} for multilayer CH_3COOH adsorption [11]. The asymmetric shape in fig. 2g at 2917 cm^{-1} with a shoulder at 2958 cm^{-1} and the off-specular spectra shown in fig. 3 leads us to tentatively assign those peaks above 2950 cm^{-1}, at large dosages, as the ν_{H-O-H} mode since ν_{C-H} is believed to be enhanced in off-specular scattering which is observed below 2950 cm^{-1} in fig. 3. However, as we have mentioned above, the assignment for this mode is not conclusive.

Comparing the coverage dependent HREEL spectra of CH_3COOH (fig. 2), CH_3COOD (fig. 5) and $^{13}CD_3COOH(D)$ (fig. 6), we have assigned the 1034 cm^{-1} band in fig. 2, the 1039 cm^{-1} band in fig. 5 and the 1039 cm^{-1} band in fig. 6 to a C–C stretching vibration. The alternative assignment of this band to out-of-plane CH_3 bending (ρ_{CH_3}) [32] or OH in plane bending (δ_{OH}) [13] dose not seem appropriate here since this peak does not show a significant shift upon deuteration of either the methyl or the hydroxyl group.

The band at ~ 1660 cm^{-1} (fig. 2d) is very weak in intensity. This mode is not detected for small dosages (figs. 2a–2c). The acetic acid isotopic adsorptions have not resulted in significant shifts of this peak. For CH_3COOD adsorption, this band is at 1631–1660 cm^{-1} and for $^{13}CD_3COOH$ adsorption, this band is at 1600–1640 cm^{-1}. Thus, we can rule out a hydrogen related vibration for this band. A possible assignment for this band is from the carbonyl stretching mode ($\nu_{C=O}$) of the acetic acid dimers since with low dosages where the surface is dominated by acetate species, this mode is not detected (figs. 2a–2c). When the acetic acid dosages exceed the dimer formation range ($\theta \sim 0.5$) this mode is observed in on-specular scattering (figs. 2d–2h, figs. 5a–5c and figs. 6b and 6c). A carbonyl stretching mode at ~ 1660 cm^{-1} has also been reported by Bellamy et al. [30] which supports our assignment.

Strong bands at ~ 1400 cm^{-1} for CH_3COOH (figs. 2d–2h), at ~ 1388 cm^{-1} for CH_3COOD (figs. 5a–5c) and at ~ 1383 cm^{-1} for $^{13}CD_3COOH(D)$ have two sources of contribution. At small dosages where acetate species dominate the surface, this band corresponds to the ν_{sCOO} mode of the acetate species. At large dosages where both acetate and acetic acid dimers are present, the δ_{CH_3} mode of the acetic acid can also contribute to this peak. We consider that the ν_{sCOO} mode of the acetate species is the major contributor for this peak due to the lack of isotope shift of this band

when methyl group is substituted by D.

Table 2 has summarized the mode assignments for molecularly adsorbed acetic acid. Our peak assignments and those of gas phase acetic acid [13] and acetic acid adsorbed on Al(111) [11] are listed as well.

4.4. Hydrogen bonding and acetic acid dimerization

In the introduction, we have mentioned our motivation for the study of acetic acid adsorption on Pt(111). Our previous studies of hydrogen bonding effects were conducted on formamide ($HCONH_2$) on Ni(111) [4] and on Pt(111) [5]. In the $HCONH_2$/Ni(111) system, hydrogen bonding has been considered to influence the adsorption geometry of the formamide molecules which leads to two parallel reaction channels. For the $HCONH_2$/Ni(111) and $HCONH_2$/Pt(111) systems, red shifts and broadening of the ν_{NH} peak are observed and a dimer form of $HCONH_2$ was proposed. In this work for the acetic acid/Pt(111) system, we also observed strong hydrogen bonding between adsorbed acetic acid species which is indicated by the presence of a substantially blue shifted γ_{OH} mode of the dimer form of acetic acid.

Hydrogen bonding in the liquid and solid phase has been extensively studied [33]. However, not much attention has been given to hydrogen bonding effects in surface adsorption and surface reactions. Apart from the $HCONH_2$/Ni(111) and CH_3COOH/Pt(111) systems in which hydrogen bonding effects are focused, Kay et al. [34] have studied H_2O, HF, and NH_3 adsorption. They have observed that hydrogen bonding could shift submonolayer TDS peaks to higher temperatures and could change the order of the desorption kinetics. Since surface chemistry mostly concerns the first monolayer of adsorbed species, the hydrogen bonding in the first monolayer appears to be more important than the hydrogen bonding formed in multilayers which has the nature of physisorption and is in many ways similar to the solid phase of the molecule. In our studies, the onset of the γ_{OH} mode at 932 cm^{-1} appears at $\theta \sim 0.5$. This mode is significantly blue shifted ($\Delta\nu \sim 282$ cm^{-1}) from the corresponding peak of the monomer (~ 650 cm^{-1}) and thus is assigned as the dimer γ_{OH} mode. This mode from the dimer

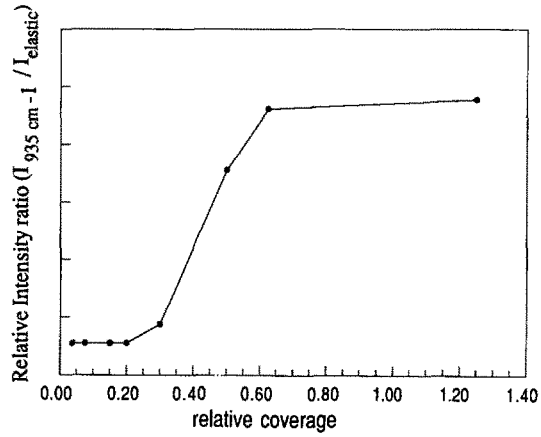

Fig. 7. The relative intensity of the γ_{OH} mode as a function of the acetic acid dosage.

Table 2
Acetic acid vibrational mode assignments.

	$CH_3COOH_{(g)}$ [32]	($CD_3COOH_{(g)}$)	$CH_3COOH_{(s)}$ [38]	($CD_3COOH_{(s)}$)	Al(111) [11]		Pt(111) [this work]	
ν_{CH}	3030	(2128)	–	(22780, 2116)	3030	(2275, 2155)	2927	(2252, 2174)
ν_{OH}	3125	(3100)	2875	(2852)	2740	(2740)	2988	(2425)
$\nu_{C=O}$	1739	(1730)	1648	(1641)	1730	(1730)	1675	(1640)
δ_{CH_3}	1387	(1075)	1439	(1035, 1055)	1400	(1050)	1400	(913)
ν_{C-O}	1282	(1220)	1284	(1287)	1350	(1310)	1318 [os,a)]	–
δ_{OH}	1186	(1156)	1418	(1404)	990	(945)	1176	(1176)
ρ_{CH_3}	–	–	1049	(920)	–	–	1034	(903)
ν_{C-C}	–	–	908	(856)	–	–	1034	(1039)
γ_{OH}	–	–	923	(920)	–	–	932	(913)

[a)] os: off-specular observation.

form of different carboxylic acid molecules has been extensively studied as indicated in the literature [3,4,29,31,35,36]. The relative intensity of the γ_{OH} mode (relative intensity to the elastic peak of incident electron beam) as a function of dosage is plotted in fig. 7. From this plot, it is deduced $\theta \sim 0.3$ is the onset of surface hydrogen bond formation. On deuteration of the hydroxyl group, the γ_{OD} mode falls into the δ_{COO} peak region as shown in figs. 5b and 5c in which the peak at 687 cm^{-1} becomes the strongest peak with large CH_3COOD dosages. We consider that the peak at 687 cm^{-1} has contributions from two sources. One is the δ_{COO} mode and the other is the γ_{OD} mode. Without the contribution of the latter, ν_{sCOO} at ~ 1398 cm^{-1} would always be the dominant peak with all dosages as is seen for CH_3COOH molecules (figs. 2a–2h). The strongest peak of $^{13}CH_3COOH(D)$ adsorption in figs. 6b and 6c is also at ~ 661 cm^{-1} which is expected since we have 57 at% D composition for the hydroxyl group. Also, the deuteration on the methyl group has removed the δ_{CH_3} contribution to the 1383 cm^{-1} band and thus the 1383 to 661 cm^{-1} peak intensity ratio is reduced.

The characteristic γ_{OH} mode for acetic acid dimers has been correlated to the strength of the hydrogen bonding energy [14] and the OH...O bond length [31]. From our results of γ_{OH} at ~ 932 cm^{-1} using this correlation we can estimate that the hydrogen bond strength ΔH to be ~ 7.3 kcal/mol (with reference to monomer γ_{OH} at 650 cm^{-1} [14]) and the $R_{O...O}$ distance to be ~ 2.68 Å.

The presence of adsorbed monomer of acetic acid is not likely since for monomer the ν_{OH} mode should be at ~ 3583 cm^{-1} and γ_{OH} mode should be at ~ 650 cm^{-1} [14]. Neither of these modes is observed in our experiment.

4.5. *Off-specular scattering and the dimer form of acetic acid*

The surface selection rule indicates that a large perpendicular dynamic dipole component will give a strong peak in specular scattering (dipole scattering). The peak intensity would decrease dramatically as a function of off-specular scattering angle. The ν_{CO} peak has been accepted as exhibiting a dipole scattering mechanism [37]. Fig. 8 plots out the variation of ν_{sCOO}, δ_{COO} and ν_{CH} peak intensities relative to the ν_{CO} peak intensity as a function of off-specular angle when all of these modes are present for CH_3COOH adsorption. It can be seen that as the off-specular angle increases, the ν_{sCOO} and δ_{COO} peak intensities drop even faster than that of the ν_{CO} peak indicating that δ_{COO} and ν_{sCOO} peaks are dominated by dipole scattering. The ν_{CH} peak shows intensity enhancement relative to the ν_{CO} peak with increasing off-specular angle suggesting that the ν_{CH} peak

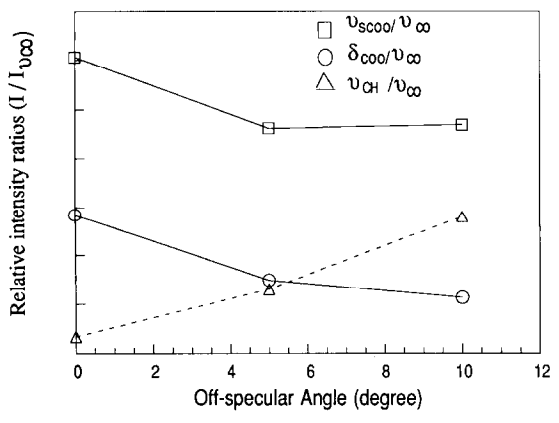

Fig. 8. The relative intensities of the ν_{sCOO}, δ_{sCOO} and ν_{CH} modes as a function of the off-specular angle.

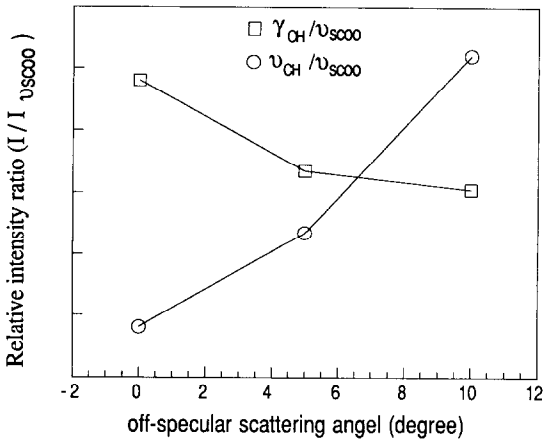

Fig. 9. The relative intensity ratios of γ_{OH}/ν_{sCOO} and ν_{CH}/ν_{sCOO} as a function of the off-specular angle.

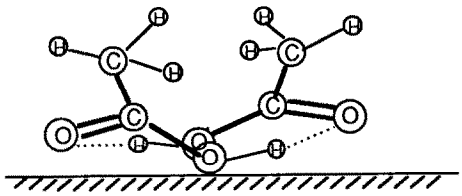

Fig. 10. Proposed cyclic acetic acid dimer adsorption configuration.

is dominated by the impact scattering mechanism. This is consistent with the general conclusion that the ν_{CH} mode has a property of off-specular enhancement [37]. Fig. 9 is a plot of both γ_{OH} and ν_{CH} peak intensities relative to the dipole dominant ν_{sCOO} peak intensity as a function of off-specular angle. The decrease of γ_{OH} peak versus ν_{sCOO} peak intensity ratio with off-specular scattering angle indicates that the OH out-of-plane bending mode is also dominated by dipole scattering. This implies that the OH bending motion should have a strong perpendicular dynamic dipole component. In fig. 10, we propose a cyclic dimer form of acetic acid adsorption configuration. This dimer form has the dimer ring nearly parallel to the metal surface and would thus give a strong perpendicular dynamic dipole component for OH out-of-plane bending motion. The C–C bond is tilted from the surface normal which agrees with the weak on-specular ν_{CC} peak (~ 1035 cm^{-1}) and possibly the weak on-specular CH bond related modes. This configuration can also account for the presence of a weak carbonyl stretching mode ($\nu_{C=O}$) at ~ 1660 cm^{-1} since the $\nu_{C=O}$ motion will give a nonzero but small perpendicular dynamic dipole component. The shift of the $\nu_{C=O}$ mode from 1717 to 1660 cm^{-1} in the temperature dependent liquid CH_3COOH IR spectra has been interpreted as a systematic change from the open chain form to the cyclic dimer form [30] which is consistent with our proposed cyclic dimer form of acetic acid adsorption. While a chain form of hydrogen-bonded acetic acid is possible, the HREEL spectra of our experiment favor the cyclic dimer by comparison with the results of the known cyclic dimer IR spectra [30,31]. The onset of the dimer formation below monolayer coverage suggests that hydrogen bonding between the acetic acid molecule and acetate species is also possible, and the configuration of which would be similar to the cyclic dimer configuration in fig. 10 with one of the H atom removed and all the rest of the configurations retained.

5. Summary

(1) CH_3COOH, CH_3COOD and $^{13}CD_3COOH$ adsorption on Pt(111) at 168 K has been studied. The vibrational mode assignments are helped by isotope substitutions on both the methyl and the hydroxyl group of the acetic acid molecules leading to the mode assignments listed in tables 1 and 2.

(2) Acetic acid adsorption on Pt(111) at 168 K exhibits both dissociative and non-dissociative adsorption. At very low dosage ($\theta \sim 0.04$), CH_3COOH dissociates into surface acetate species in an $\eta^2_{(O,O)}$-CH_3COO configuration. The acetate species can further decompose into $CO_{(a)}$, $O_{(a)}$ and $CH_{x(a)}$ species with $x = 1$–2.

(3) The acetate species ($CH_3COO_{(a)}$) is distinguishable from the formate species ($HCOO_{(a)}$) with their vibrational spectra. The former species has ν_{sCOO} mode at $1398 \sim 1470$ cm^{-1} and δ_{COO} at $650 \sim 675$ cm^{-1} while the latter species has ν_{sCOO} mode at ~ 100 cm^{-1} lower and the δ_{COO} mode at ~ 100 cm^{-1} higher than the corresponding mode for the former species.

(4) The onset of nondissociative molecular adsorption at acetic acid at 168 K is estimated to occur substantially at $\theta \sim 0.4$ which is below the monolayer coverage. It is characterized by the OH out-of-plane bending mode of the acetic acid dimer at ~ 932 cm^{-1}.

(5) The hydrogen-bonded dimer configuration is proposed which fits the HREEL spectra characteristics. The hydrogen bonding strength of the dimer ΔH is estimated to be ~ 7.3 kcal/mol and the $R_{O\ldots O}$ distance for hydrogen bonded dimer acetic acid is estimated to be ~ 2.68 Å.

Acknowledgements

This work was supported in part by the Office of Naval Research.

References

[1] R.T. Morrison, Organic Chemistry, 4th ed. (Allyn and Bacon, Boston, 1983) p. 778.
[2] P.-G. Jönsson, Acta Cryst. B 27 (1971) 893.
[3] R.E. Jones and D.H. Templeton, Acta Cryst. 11 (1958) 484.
[4] Q. Gao, W. Erley, D. Sander, H. Ibach and J.C. Hemminger, J. Phys. Chem., in press.
[5] C.F. Flores, Q. Gao and J.C. Hemminger, Surf. Sci. 239 (1990) 156.
[6] N.R. Avery, J. Vac. Sci. Technol. 20 (1982) 592.
[7] B.A. Sexton, J. Vac. Sci. Technol. 17 (1980) 141.
[8] B.A. Sexton, Chem. Phys. Lett. 65 (1979) 469.
[9] G.R. Schoofs and J.B. Benziger, Surf. Sci. 143 (1984) 359.
[10] M. Bowker and R.J. Madix, Appl. Surf. Sci. 8 (1981) 299.
[11] J.G. Chen, J.E. Crowell and J.T. Yates, Jr., Surf. Sci. 172 (1986) 733.
[12] TDS results show the onset of desorption from a multilayer film at dosing time of ~ 20 s under these experimental conditions.
[13] R.C. Herman and R. Hofstadter, J. Chem. Phys. 6 (1938) 534; 7 (1939) 460.
[14] M. Sh. Rosenberg, A.V. logansen, A.A. Mashkovsky and S.E. Odinokov, Spectrosc. Lett. 5 (1972) 75.
[15] J.E. Crowell, J.G. Chen and J.T. Yates, Jr., J. Chem. Phys. 85 (1986) 3111.
[16] R.J. Madix, J.L. Gland, G.E. Mitchell and B.A. Sexton, Surf. Sci. 125 (1983) 481.
[17] B.A. Sexton, Surf. Sci. 88 (1979) 319.
[18] S.L. Miles, S.L. Bernasek and J.L. Gland, Surf. Sci. 127 (1983) 271.
[19] N.R. Avery, B.H. Toby, A.B. Anton and W.H. Weinberg, Surf. Sci. 122 (1982) L574.
[20] B.A. Sexton and R.J. Madix, Surf. Sci. 105 (1981) 177.
[21] N.R. Avery, Appl. Surf. Sci. 11/12 (1982) 774; 14 (1982/83) 149.
[22] P. Hofmann, S.R. Bare, N.V. Richardson and D.A. King, Surf. Sci. 133 (1983) L459.
[23] Y. Zhou, M.A. Henderson and J.M. White, Surf. Sci. 221 (1989) 160.
[24] M.B. Lee, Q.Y. Yang, S.L. Tang and S.T. Ceyer, J. Chem. Phys. 85 (1986) 1693.
[25] P.M. George, N.R. Avery, W.H. Weinberg and F.N. Tebbe, J. Am. Chem. Soc. 105 (1983) 1393.
[26] J.E. Demuth and H. Ibach, Surf. Sci. 89 (1979) 425.
[27] M.B. Lee, Q.Y. Yang and S.T. Ceyer, J. Chem. Phys. 87 (1987) 2724.
[28] K.G. Lloyd, PhD Thesis, University of California, Irvine (1986) p. 148.
[29] M. Hauric and A. Novak, J. Chim. Phys. 62 (1965) 137; in: Structure of Bonding, Vol. 18, Ed. J.D. Dunitz (Springer, Berlin, 1974) p. 180.
[30] L.J. Bellamy, R.F. Lake and R.J. Pace, Spectrochim. Acta 19 (1963) 443.
[31] I. Fischmeister, Spectrochim. Acta 20 (1964) 1071.
[32] K. Ito and H.J. Bernstein, Can. J. Chem. 34 (1956) 170.
[33] P. Schuster, G. Zundel and C. Sandorfy, Ed., The Hydrogen Bond, Vols. 1–3 (North-Holland, Amsterdam, 1976).
[34] B.D. Kay, K.R. Lykke, J.R. Creighton and S.J. Ward, J. Chem. Phys. 91 (1989) 5120.
[35] D. Hadzi, B. Orel and A. Novak, Spectrochim. Acta 29 A (1973) 1745.
[36] A. Novak, Structure and Bonding, Vol. 18, Ed. J.D. Dunitz (Springer, Berlin, 1974) p. 177.
[37] H. Ibach and D.L. Mills, Eds., Electron Energy Loss Spectroscopy and Surface Vibrations, (Academic Press, New York, 1982).
[38] M. Haurie and A. Novak, Spectrochim. Acta 21 (1965) 1217.